

**$T = 1$  states in  $^{74}\text{Rb}$  and their  $^{74}\text{Kr}$  analogs**

S. M. Fischer\*

*Department of Physics, DePaul University, Chicago, Illinois 60614, USA, and Physics Division, Argonne National Laboratory, Argonne, Illinois 60439, USA*C. J. Lister, N. J. Hammond, R. V. F. Janssens, T. L. Khoo, T. Lauritsen, E. F. Moore,  
D. Seweryniak, and S. Sinha*Physics Division, Argonne National Laboratory, Argonne, Illinois 60439, USA*

D. P. Balamuth and P. A. Hausladen

*Department of Physics and Astronomy, University of Pennsylvania, Philadelphia, Pennsylvania 19104, USA*

D. G. Sarantites and W. Reviol

*Department of Chemistry, Washington University, St. Louis, Missouri 63130, USA*

P. Chowdhury

*Department of Physics, University of Massachusetts Lowell, Lowell, Massachusetts 01854, USA*

S. D. Paul, C. Baktash, and C.-H. Yu

*Physics Division, Oak Ridge National Laboratory, Oak Ridge, Tennessee 37831, USA*

(Received 28 July 2006; published 10 November 2006)

Charge symmetry breaking effects that perturb analog symmetry between nuclei are usually small but are important in extracting reliable Fermi matrix elements from “superallowed”  $\beta$  decays and testing conserved vector current theory, especially for the heavier cases. We have used the  $^{40}\text{Ca}(^{36}\text{Ar}, pn)^{74}\text{Rb}$  and  $^{40}\text{Ca}(^{40}\text{Ca}, \alpha pn)^{74}\text{Rb}$  reactions at 108, 123 and 160 MeV, respectively, to populate  $^{74}\text{Rb}$  and determine the analog distortion through comparison of  $T = 1$  states in  $^{74}\text{Rb}$  with their corresponding  $^{74}\text{Kr}$  levels. We have traced the analogs of the  $^{74}\text{Kr}$  ground-state band in  $^{74}\text{Rb}$  to a candidate spin  $J = 8$  state and determined the Coulomb energy differences. They are small and positive and increase smoothly with spin. New  $T = 0$  states were found that better delineate the deformed band structure and clarify the steps in deexcitation from high spin. A new  $T = 0$  band was found. No evidence was found for  $\gamma$  decay to or from a low-lying  $J^\pi = 0^+$  state in  $^{74}\text{Rb}$  despite a careful search.

DOI: [10.1103/PhysRevC.74.054304](https://doi.org/10.1103/PhysRevC.74.054304)

PACS number(s): 27.50.+e, 23.20.Lv, 23.20.En, 21.10.Hw

**I. INTRODUCTION**

Charge symmetry breaking effects that perturb analog symmetry between nuclear states are interesting, but usually small, at the level of tens of keV, except for special cases [1–6]. Along the  $N = Z$  line these effects arise from binding energy differences, Coulomb distortion, and the electromagnetic spin-orbit interaction, all of which grow with mass to a level where they can become significant in defining the structure of nuclei. These effects are of special interest as they are important in extracting Fermi matrix elements from “superallowed”  $\beta$  decays and testing conserved vector current (CVC) theory [7,8]. For  $\beta$  decay, the key requirement is a good description of the ground-state wave functions or, more particularly, the difference in wave functions between parent and daughter nuclei. One issue is the admixture of excited state configurations into the ground states. In the nuclei of greatest interest for precise CVC tests, the decays are from  $J^\pi = 0^+$ ,  $T = 1$ ,  $T_z = 0$  odd-odd nuclei to their  $T = 1$ ,  $T_z = 1$  even-even daughters. A key issue is the location

of excited  $J^\pi = 0^+$  states that can mix with the ground states, especially if the mixing is different in parent and daughter. In  $A \sim 74$  this is a particularly important issue as there are known excited  $J^\pi = 0^+$  states at only  $\sim 500$  keV, arising from shape coexistence. Low-lying isomers are known in  $^{72,74}\text{Kr}$  [9,10], but the analog counterpart in  $^{74}\text{Rb}$  has not yet been found despite many searches [11–15]. Thus, it is an experimental challenge to ascertain where the  $T = 1$  levels are in  $^{74}\text{Rb}$ , measure the Coulomb shifts, and determine the location of the isomer. It is a timely question, as  $^{74}\text{Rb}$  lies beyond the reach of current full shell-model calculations, so it is important to provide new data to test the current truncated calculations [16]. In addition, the odd-odd nuclei are important in this mass region for ascertaining the strength of  $T = 1$  neutron-proton ( $np$ ) pairing and, indeed, for seeking evidence for deuteron-like  $T = 0$  correlations [14,15,17–22].

In  $\beta$ -decay studies of  $^{74}\text{Rb}$ , two groups reported precise half-life determinations [13,23]. A direct mass difference measurement was made using trapped ions [24]. Branches to excited states in  $^{74}\text{Kr}$  were seen and measured [25,26], completing the key observations needed to precisely determine the  $\log ft$  value.  $^{74}\text{Kr}$  was extensively studied “in-beam” [27,28]. Most importantly, a long-lived  $J^\pi = 0^+$  low-lying

\*Electronic address: [sfischer@depaul.edu](mailto:sfischer@depaul.edu)

TABLE I. Description of the three experiments used to study excited states in  $^{74}\text{Rb}$ . The experiments are categorized according to the reaction, beam energy, target thickness, average beam current, time duration of data collection, number of Gammasphere (GS) HPGe detectors, and the type of auxilliary detectors used.

Experiment	Reaction	$E_{\text{beam}}$ (MeV)	Target ( $\mu\text{g}/\text{cm}^2$ )	$I_{\text{avg}}$ (pnA)	Time (hr)	GS detectors	Auxilliary detectors
GSFMA19	$^{40}\text{Ca}(^{40}\text{Ca}, \alpha pn)$	160	500	3.2	48	86	20 neutron detectors <sup>a</sup> + Microball
GSFMA77	$^{40}\text{Ca}(^{40}\text{Ca}, \alpha pn)$	123	1030	2.5	66	78	30 neutron detectors <sup>b</sup> + Microball
GSFMA123	$^{40}\text{Ca}(^{36}\text{Ar}, pn)$	108	600	5.0	98	76	26 neutron detectors <sup>b</sup> + FMA

<sup>a</sup>A collection of scintillators from the University of Manchester and the University of Pennsylvania.

<sup>b</sup>Washington University neutron shell.

shape isomer was found at 508 keV [9] and its decay modes studied [10]. Excited states based on this isomer were found [29]. Excited states were first identified in  $^{74}\text{Rb}$  by Rudolph *et al.* [14]. They suggested that strong neutron-proton correlations were responsible for lowering the  $T = 1$  levels relative to the  $T = 0$  states. This effect is now found to be a ubiquitous feature in odd-odd  $N = Z$  nuclei in this region [21,22], with similar ( $T = 1$ )-( $T = 0$ ) gaps of  $\sim 1$  MeV. However, with the sensitivity of the original experiment, only the ground state and  $T = 1$ ,  $J^\pi = 2^+, 4^+$  states were identified. Higher lying  $T = 1$  levels were not observed, as  $J = \text{odd } T = 0$  levels form the yrast sequence and take most of the population. A more recent study [15] extended the decay scheme to high spin but has not advanced the knowledge of the important  $T = 1$  levels.

In this article we present new data from three different experiments that extend the structural knowledge of  $^{74}\text{Rb}$ . The  $T = 0$  portion of the decay scheme was considerably extended. Two of the experiments were directly aimed at the challenge of populating nonyrast, low-spin levels, which are very difficult to reach with heavy ions. However, both for CVC tests and for understanding  $np$  pairing, it is these low-spin levels in  $N = Z$  nuclei that are most important.

## II. THE EXPERIMENTS

Three studies to produce excited states in  $^{74}\text{Rb}$  were performed at the ATLAS facility at Argonne National Laboratory using the Gammasphere array [30] to detect  $\gamma$  rays emitted following either the  $^{40}\text{Ca}(^{40}\text{Ca}, \alpha pn)$  or the  $^{40}\text{Ca}(^{36}\text{Ar}, pn)$  reaction. Different techniques were used to correlate the observed  $\gamma$  rays with the proper nucleus. In two of the studies, the reaction channels were identified by detecting the emitted protons and  $\alpha$  particles with the Microball array [31] and using an array of liquid scintillators [32] to detect the neutrons. In the other study, the recoiling nuclei were selected by the Argonne Fragment Mass Analyzer (FMA) [33] according to their charge to mass ratio and could be further selected through the identification of an evaporated neutron. Details of the three studies are contained in Table I.

The decay scheme for  $^{74}\text{Rb}$  deduced from these data is shown in Fig. 1. The relative intensities of the transitions, as depicted through the thickness of the arrows, correspond

primarily to those observed in the high-spin study of  $^{40}\text{Ca}(^{40}\text{Ca}, \alpha pn)$  at 160 MeV. Transitions observed in the low-spin studies are also included in the figure. Table II contains detailed information about the data, including a comparison of the relative intensities of the transitions observed in the three studies. Note that the intensities are normalized relative to the 528-keV transition, rather than to the intensity of the 478-keV,  $2^+ \rightarrow 0^+$  transition, due to the difficulty in obtaining clean ‘‘singles’’ spectra in some of the data sets. The difference in the relative population in the various reactions of the 2309-keV state, which decays via the 303-keV transition, is quite striking, being more than a factor of 2 larger for the Ca + Ca study at 160 MeV versus that at 123 MeV. Although this dependence on beam energy is not terribly surprising, a similar comparison of relative intensities of the 783-keV transition from the state at 1836 keV shows that this  $6^+$  state is populated with reasonable intensity at the lower beam energies, but was unobserved at the higher energy. This exemplifies the difficulty in experimentally populating such nonyrast states.

Gamma-ray transitions and level energies were determined through a variety of coincidence analyses for the different data sets. When evaporated particles were used for channel selection,  $\gamma$  rays were required to be in coincidence with the detection of 1 proton, 1  $\alpha$ , and 1 neutron and to ‘‘survive’’ the subtraction of background due to the presence of the  $\alpha 2pn$  channel. When the recoiling nuclei were detected using the FMA,  $\gamma$  rays were required to be in coincidence with a mass 74 recoil along with the detection of one neutron. After this identification,  $\gamma\gamma + \alpha pn$  coincidences were analyzed for both  $^{40}\text{Ca} + ^{40}\text{Ca}$  data sets, along with  $\gamma\gamma + (A = 74)$  coincidences for the  $^{36}\text{Ar} + ^{40}\text{Ca}$  data. In addition, a  $\gamma$ -ray triples analysis of the  $^{40}\text{Ca} + ^{40}\text{Ca}$  data at 160 MeV, with the requirement that the  $\gamma$  rays were in coincidence with the detection of one proton and one  $\alpha$ , provided the greatest statistics, and allowed for the level scheme to be extended to higher spin. Several analyses to extract  $\gamma$ -ray angular distributions were also performed. The results are presented in Table II and Fig. 2, with details provided in the figure caption.

A comparison should be made between the decay scheme in this work (Fig. 1) and those of the earlier works of Rudolph *et al.* [14] and O’Leary *et al.* [15]. We have followed the nomenclature of the bands from Ref. [15] to make this comparison more straightforward. In the first observation of

TABLE II. The excited states of  $^{74}\text{Rb}$ , the transition energies and relative intensities of the  $\gamma$  rays observed in the various experiments (GSFMA19, GSFMA77, and GSFMA123), and the spins and parities of the initial and final states. The  $\delta(E2/M1)$  mixing ratios are average values determined from angular distribution measurements. Tentative  $\gamma$  rays and levels are included in the table and can be identified as dashed lines in Fig. 1. See Table I for a description of the three experiments.

$E_x$ (keV)	$E_\gamma$ (keV)	$J_i^\pi$	$J_f^\pi$	GSFMA19 $I_\gamma$	GSFMA77 $I_\gamma$	GSFMA123 $I_\gamma$	Multipole assignment	$\delta$
477.8(2)	477.8(2)	2 <sup>+</sup>	0 <sup>+</sup>	222(9)	~300	240(40)	E2	
921.0(5)	443.2(5)		2 <sup>+</sup>	34(9)	27(4)	23(9)		
1005.4(3)	527.6(2)	3 <sup>+</sup>	2 <sup>+</sup>	100(5)	100(8)	100(13)	M1/E2	0.15(8)
1052.9(5)	575.1(4)	4 <sup>+</sup>	2 <sup>+</sup>	72(5)	94(17)	53(15)	E2	
1169.3(7)	248.3(4)			17(9)	10(3)	4(2)		
1222.9(4)	217.5(2)	4 <sup>+</sup>	3 <sup>+</sup>	38(3)	34(4)	34(6)	M1/E2	0.01(13)
1364.1(7)	311.2(5)			16(3)	15(3)	15(6)		
1487.3(3)	264.3(4)	5 <sup>+</sup>	4 <sup>+</sup>	21(3)	12(3)	11(4)	M1/E2	0.30(21)
	481.9(2)	5 <sup>+</sup>	3 <sup>+</sup>	81(7)	53(6)	60(11)	E2	
1544.3(5)	491.4(3)	6 <sup>+</sup>	4 <sup>+</sup>	31(3)	14(3)	30(9)	E2	
1801.1(5)	578.2(3)		4 <sup>+</sup>	16(5)	21(7)	21(11)		
1805(1)	636(1)			26(5)		23(6)	E2	
1836.0(8)	783.1(6)	6 <sup>+</sup>	4 <sup>+</sup>		26(5)	23(9)	E2	
1930(1)	707(1)				12(5)			
2006.7(4)	519.4(2)	7 <sup>+</sup>	5 <sup>+</sup>	81(5)	35(5)	36(9)	E2	
2203(1)	716(1)			8(4)				
2238.0(7)	693.7(5)	8 <sup>+</sup>	6 <sup>+</sup>	31(3)	12(3)	13(6)	E2	
2309.4(4)	302.7(2)	9 <sup>+</sup>	7 <sup>+</sup>	86(5)	35(4)	47(9)	E2	
2341.0(8)	539.9(6)				11(3)			
2367.4(9)	531.4(5)				9(6)			
2618(2)	813(1)			31(10)		17(9)	E2	
2631.6(5)	624.9(3) <sup>a</sup>			34(5)	30(5)	47(11)		
2812(2)	976(2)	(8 <sup>+</sup> )	6 <sup>+</sup>			<5		
2967.3(8)	729.8(4)	(10 <sup>+</sup> )	8 <sup>+</sup>	26(8)				
3132.7(5)	823.3(2)	11 <sup>+</sup>	9 <sup>+</sup>	71(5)	26(4)	40(11)	E2	
3592(2)	974(1)			16(5)		30(11)	E2	
3851.5(9)	884.2(4)	(12 <sup>+</sup> )	(10 <sup>+</sup> )	26(8)				
4085.6(5)	952.9(2)	13 <sup>+</sup>	11 <sup>+</sup>	60(5)		30(9)	E2	
4729(3)	1137(2)							
4902.3(10)	1050.8(5)	(14 <sup>+</sup> )	(12 <sup>+</sup> )	22(6)				
5209.9(7)	1124.3(5)	15 <sup>+</sup>	13 <sup>+</sup>	50(5)		34(9)	E2	
5981(3)	1252(2)							
6083.9(12)	1181.6(7)	(16 <sup>+</sup> )	(14 <sup>+</sup> )	21(6)				
6510.5(9)	1300.6(6)	(17 <sup>+</sup> )	15 <sup>+</sup>	50(5)				
7412(2)	1328(1)	(18 <sup>+</sup> )	(16 <sup>+</sup> )	18(5)				
7436(5)	1455(3)							
7998(2)	1487(1)	(19 <sup>+</sup> )	(17 <sup>+</sup> )	50(5)				
8916(3)	1504(2)	(20 <sup>+</sup> )	(18 <sup>+</sup> )	15(8)				
9070(6)	1634(4)							
9645(3)	1647(2)	(21 <sup>+</sup> )	(19 <sup>+</sup> )	38(5)				
11398(4)	1753(3)	(23 <sup>+</sup> )	(21 <sup>+</sup> )	17(5)				
13359(5)	1961(3)	(25 <sup>+</sup> )	(23 <sup>+</sup> )	17(5)				
—	343(1) <sup>b</sup>			<10				
—	475.3(3) <sup>b</sup>				19(4)			

<sup>a</sup> $\gamma$  ray appears to be a doublet.

<sup>b</sup> $\gamma$  ray is unplaced in the decay scheme.

excited states in  $^{74}\text{Rb}$ , Rudolph *et al.* [14] identified the first two excited states of the ground-state band (band 1 in Fig. 1), states in band 4 to an excitation energy of ~6515 keV, and the 578-keV transition of band 2. O'Leary *et al.* [15] confirmed this level scheme and extended band 4 to a tentative

spin of (31<sup>+</sup>) at 21612 keV. Band 4 of the current study is in general agreement with the O'Leary [15] and Rudolph [14] works, with a reversal in placement of the 303- and 519-keV transitions, as discussed below. However, there appears to be a fairly systematic difference in the transition energies, with

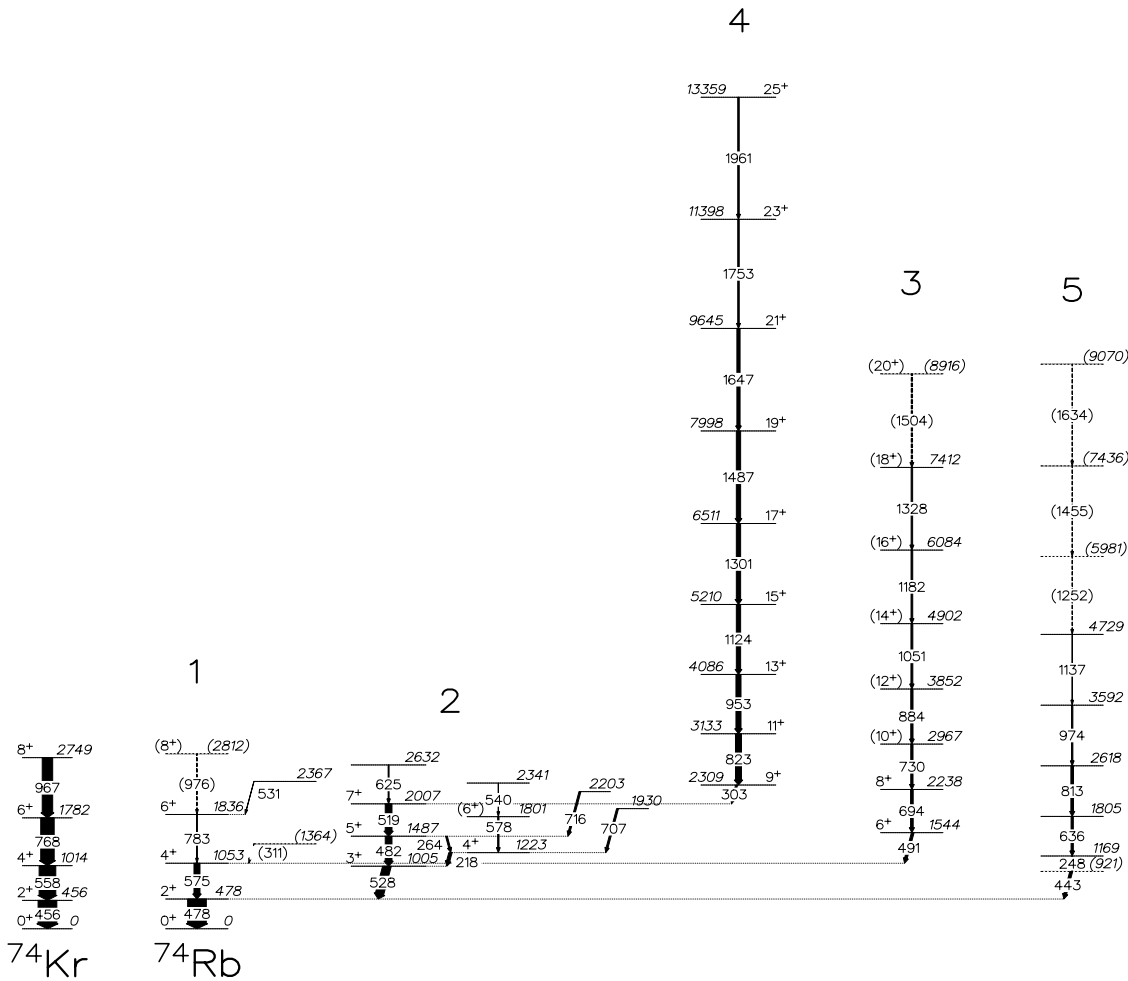


FIG. 1. The composite decay scheme for  $^{74}\text{Rb}$  inferred from this work. The band numbering follows that of Ref. [15]. The  $\gamma$ -ray intensities, as indicated by the widths of the arrows, are taken primarily from the  $^{40}\text{Ca} + ^{40}\text{Ca}$  study at 160 MeV. A portion of the ground-state band for the isobar  $^{74}\text{Kr}$  is shown at the left, with relative  $\gamma$ -ray intensities taken from the high-spin study of Rudolph *et al.* [28].

many of the energies of this work 1–2 keV lower than those given by O’Leary *et al.* [15]. Gamma rays from the  $\alpha p$  and  $\alpha 2p$  channels ( $^{75}\text{Rb}$  and  $^{74}\text{Kr}$ ) also occur in the  $\gamma$ -ray triples data for events coincident with the detection of one  $\alpha$  and one proton. The energies of these  $\gamma$  rays in our analysis were found to be consistent within uncertainty to those in the literature for  $^{75}\text{Rb}$  [34] and  $^{74}\text{Kr}$  [28].

In the previous studies [14,15], band 4 was populated at reasonably high spin and excitation energy, resulting in a fairly constant intensity of  $\gamma$  rays within the band for transitions decaying out of states of  $J = 11$  to  $J = 7$  [14] and states of  $J = 19$  to  $J = 7$  [15]. The ordering of these transitions can thus not be determined through measured intensities. Our data suggest a reversal in placement of the 303- and 519-keV transitions based on the observation of a 625-keV transition that is coincident with the 519-keV transition and appears to be in parallel with the 303-keV transition, as shown in Fig. 1. Four relevant spectra are displayed in Fig. 3. These spectra were obtained from the low-energy  $^{40}\text{Ca} + ^{40}\text{Ca}$  data set, but analogous spectra from the  $^{36}\text{Ar} + ^{40}\text{Ca}$  data confirm these relationships. Figure 3(a) shows a gate on the 528-keV

transition from the state at 1005 keV. Note the slightly larger intensity of the 519-keV transition as compared with the 303-keV transition, as well as the presence of the 625-keV  $\gamma$  ray. Figure 3(b) is the result of a 625-keV gate. The 519-keV  $\gamma$  ray is evident, whereas there is no indication of a  $\gamma$  ray at 303 keV. A 488-keV transition is present in both of the low-spin data sets but could not be confidently placed. The 417-keV  $\gamma$  ray does not appear in the  $^{36}\text{Ar} + ^{40}\text{Ca}$  data set. The presence of the 636-keV peak suggests that the 625-keV  $\gamma$  ray may be a doublet, with a second transition in coincidence with transitions in band 3. Supporting this is the appearance of a 625-keV transition in sums of double gates involving  $\gamma$  rays belonging to band 3, as shown in the upper panel of Fig. 4. Returning to Fig. 3, panel (c) shows the 519-keV gate, with a pronounced peak at 625 keV, whereas panel (d) shows the 303-keV gate. The 575-keV coincident  $\gamma$  ray appears in the 303-keV gate only in this data set and may indicate the presence of an additional transition of energy  $\sim 303$  keV. The reactions at lower beam energy clearly populate low-energy, nonyrast states that are simply bypassed in the higher energy reactions.

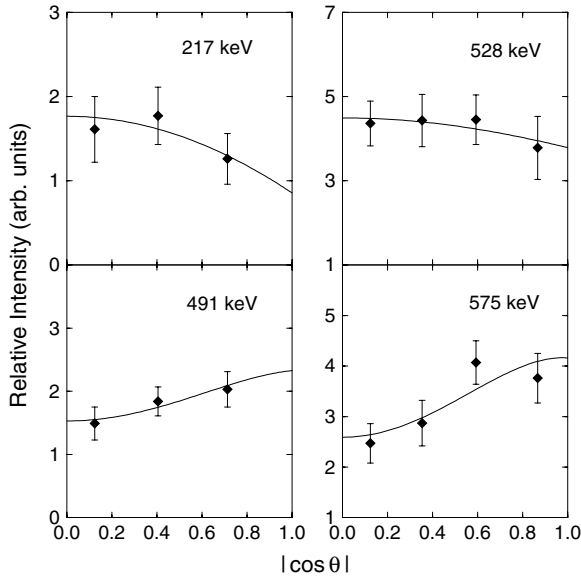


FIG. 2. Sample  $\gamma$ -ray angular distributions obtained from the  $^{40}\text{Ca} + ^{40}\text{Ca}$  160-MeV data set. Due to the low production cross section for  $^{74}\text{Rb}$ , the data from neighboring rings of Gammasphere detectors were added together to improve the statistics as a function of angle. The data in the panels on the left were obtained from  $\gamma$ -gated spectra correlated with the detection of one proton and one  $\alpha$  in the Microball array. The data in the panels on the right were obtained from  $\gamma$ -ray “singles” spectra coincident with the detection of one proton, one  $\alpha$ , and one neutron. The solid curves represent fits to the data assuming an alignment of  $\sigma/J = 0.35$ , and with the spins as shown in Table II.

Allowing for the reordering of these two transitions, our spin assignments for bands 2 and 4 agree with those of O’Leary *et al.* [15]; we have adopted a firm positive parity assignment for the  $3^+$  level at 1005 keV following the measurement of the angular distribution of the 528-keV transition in three different analyses, one of which is shown in Fig. 2. The average value of the mixing ratio,  $\delta(E2/M1) = 0.15(8)$ , favors the same parity for the initial and final states. The  $^{40}\text{Ca} + ^{40}\text{Ca}$  reaction at the lower beam energy allowed for the population of the additional state at 2341 keV in band 2.

O’Leary *et al.* [15] observed band 3 to a spin of  $(22^+)$ , including the same set of  $\gamma$  rays reported in this work. However, the 730-keV transition from the  $(10^+)$  state in our Fig. 1 was placed as a tentative transition at a similar location but not as a member of band 3. Instead, O’Leary *et al.* [15] identified the 884-keV transition as decaying from the  $(10^+)$  state. The lower panel of Fig. 4 shows a spectrum resulting from a sum of  $\gamma\gamma$  gates applied to the high-spin data, as discussed earlier. Each gate consists of one transition below the  $8^+$  state at 2238 keV and one transition above the  $(10^+)$  state at 2967 keV. The resulting spectrum clearly shows a transition of energy 730 keV. In addition,  $\gamma\gamma$  gates involving the 730-keV  $\gamma$  ray along with the 478-, 491- or 694-keV  $\gamma$  rays show a peak at 884 keV, indicating that the 730-keV transition is a member of the band. Analysis of other data sets suggests that the intensity of the 730-keV transition is somewhat weaker than would be expected from a simple cascade of decays,

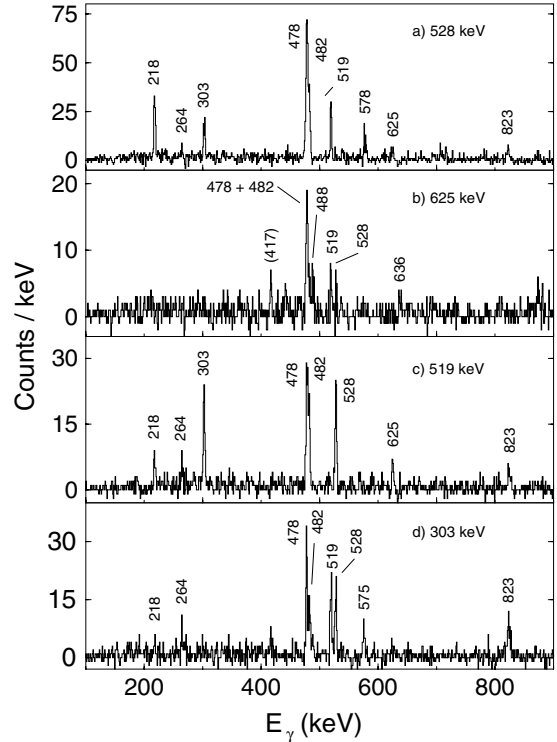


FIG. 3. Spectra showing  $\gamma$  rays in coincidence with the particular  $\gamma$ -ray transition indicated in each panel. The data are from the  $^{40}\text{Ca} + ^{40}\text{Ca}$  study at 123 MeV. This set of spectra is provided to support the revised placement of the 303- and 519-keV transitions of  $^{74}\text{Rb}$ .

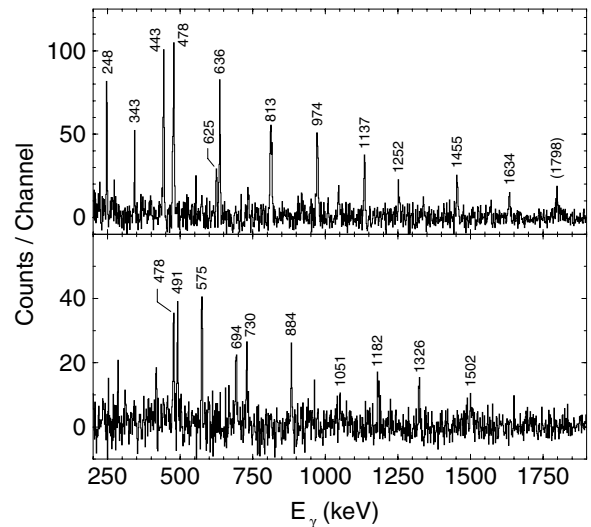


FIG. 4. Gamma-ray spectra obtained from the addition of selected  $\gamma\gamma$  gates applied to the  $^{40}\text{Ca} + ^{40}\text{Ca}$  at 160-MeV data set. The upper panel shows the sum of all double gates involving the 443-, 248-, 636-, 813- or 974-keV transitions of band 5. The lower panel focuses on band 3 and shows the sum of double gates in which one gate belongs to the set of (478-, 491-, and 694-keV) transitions and the second gate to the set of (884-, 1051-, and 1182-keV) transitions. The presence of the 730-keV  $\gamma$  ray indicates that it is also a member of band 3.



indicating that perhaps there is some other decay out of band 3 to unidentified states [35].

Band 5, as shown in the upper panel of Fig. 4, is new in this work. This band is populated with a slightly larger intensity than band 3 in the high-spin data set and, by chance, it suffers from fewer similarities with  $\gamma$  rays in contaminant reaction channels, allowing for cleaner spectra to be produced. It is likely that the nonobservation of this band by O’Leary *et al.* [15] is due to its having only one transition in common with the decay scheme of Rudolph *et al.* [14], making discovery by  $\gamma$ -triples analysis extremely difficult. In our study, several transitions in the new band could be first identified in  $\gamma$ -ray singles or doubles data that were directly associated with  $^{74}\text{Rb}$ . The O’Leary *et al.* [15] work employed only charged particle detection and did not include neutron identification, so the firm assignment of new transitions to  $^{74}\text{Rb}$  in lower fold data was not possible.

The ordering of the 443- and 248-keV transitions at the bottom of the band along with the assignment of spin and parity to the associated levels is problematic. In all data sets, the 443-keV transition is significantly more intense than the 248-keV transition, suggesting that the 443-keV transition should be placed lower in the decay scheme. However, the 636-keV transition from the state at 1805 keV is consistently more intense than the 248-keV transition. In addition, the 248-keV transition is clearly in coincidence with all other transitions firmly placed in band 5, making it unlikely that the  $\gamma$  ray feeds into the band from the side. If the 248-keV transition is placed below the 443-keV transition, the “missing” intensity must be accounted for. Internal conversion cannot account for the low intensity of the  $\gamma$  ray, and the data show no evidence for an additional 726-keV transition directly to the ground state. It is possible that the 248-keV  $\gamma$  ray decays out of an isomer with a half-life on the order of tens of ns, with a resulting loss of efficiency due to emission away from the target position. In a previous analysis [36] it was possible to observe delayed  $\gamma$  rays from 20- to 30-ns isomers that could be correlated with the emission of prompt charged particles and neutrons, and that showed no Doppler shifts because the nuclei had come to rest on the absorbers covering the Microball detectors. The current experiments showed no evidence for any delayed  $\gamma$  rays in  $^{74}\text{Rb}$ . The angular distribution data, although having poor statistics, indicate a probable  $L = 2$  character for the 443-keV transition and show an isotropic distribution for the 248-keV transition. The “flatness” of the distribution could come from a loss of alignment due to the presence of an isomer or to the nature of the particular  $J_i \rightarrow J_f$  decay, for example, an  $E2/M1$  decay with a large mixing ratio. Angular distributions for the 636-, 813- and 974-keV  $\gamma$  rays in band 5 indicate that these are  $L = 2$  transitions.

We have been able to follow the analogs of the ground-state band in  $^{74}\text{Kr}$ . One new transition, the  $6^+ \rightarrow 4^+$  has been unambiguously placed. Figure 5 shows the  $\gamma$ -ray spectrum observed in coincidence with the 783-keV transition. The  $4^+ \rightarrow 2^+$  and  $2^+ \rightarrow 0^+$  transitions are clearly evident. The population of this band drops rapidly as it grows increasingly nonyrast. However, a candidate  $8^+ \rightarrow 6^+$  transition of 976(2) keV was found in the  $^{36}\text{Ar} + ^{40}\text{Ca}$  data but this was quite weak.

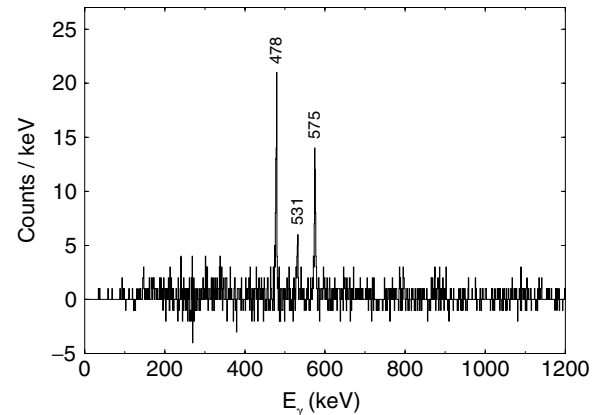


FIG. 5. Gamma-ray spectrum resulting from a gate on the 783-keV transition from the  $6^+$  state at 1836 keV in  $^{74}\text{Rb}$ . The spectrum was obtained from the  $^{40}\text{Ca} + ^{40}\text{Ca}$  at 123-MeV data set.

In more neutron-rich odd-odd rubidium isotopes there is a very large level density at low excitation energy and many band structures are known. In  $N = Z$   $^{74}\text{Rb}$ ,  $np$  pairing lowers the  $T = 1$  ground state below all the  $T = 0$  coupled configurations [14], keeping the level density initially low and the level scheme simple. Above  $\sim 1$  MeV evidence for many new structures starts to emerge; however, the low production cross section for  $^{74}\text{Rb}$  on the order of several hundred  $\mu\text{b}$  makes experimental progress difficult. For example, a clear 531-keV transition that feeds into the  $6^+$  analog state can be seen in Fig. 5. Other  $\gamma$  rays were found to feed into various bands but were difficult to place unambiguously. For instance, 344- and 625-keV  $\gamma$  rays appear in the spectrum of band 5 in the upper panel of Fig. 4. The 344-keV transition may feed into the state at 1169 keV and the 625-keV transition appears to be a doublet, as discussed earlier.

### III. DISCUSSION

#### A. Systematics of $T = 1$ analogs

The candidate  $T = 1$  band in  $^{74}\text{Rb}$  is shown in Fig. 1 as band 1. As can be seen, it mimics the ground-state band of  $^{74}\text{Kr}$  closely. It can be followed to higher spin than counterpart analog bands in lighter  $N = Z$  odd-odd nuclei as the  $T = 1$  band head is pulled  $\sim 1$  MeV below the other states by neutron-proton correlations, leaving a “gap” in which this rotational sequence is favored.  $^{74}\text{Rb}$  is moderately deformed and the moment of inertia is large enough to compress the spectrum and allow the states to energetically compete with other configurations. Even so, these levels rapidly become nonyrast with increasing spin and become difficult to follow. However, this is the most distinct band of this type yet reported insofar as the analog levels not only lie at similar energies but also have similar decays. In lighter nuclei where there is no “gap” between  $T = 1$  and  $T = 0$  states, the  $E2$  decays of the analog band are usually in competition with faster and stronger  $\Delta T = 1$ ,  $M1$  transitions [37,38] to a point that the  $E2$  decays are very difficult to observe. Our candidate  $J = 8$  analog state is the highest known that decays by an  $E2$  cascade. The

TABLE III. Coulomb energy differences (CEDs) for the  $2^+$ ,  $4^+$ ,  $6^+$ , and  $8^+$  states, where possible, for  $T = 1$  systems above  $^{56}\text{Ni}$ .

Nuclide	$\Delta E(2^+ \rightarrow 0^+)$ (keV)	CED( $2^+$ ) (keV)	$\Delta E(4^+ \rightarrow 2^+)$ (keV)	CED( $4^+$ ) (keV)	$\Delta E(6^+ \rightarrow 4^+)$ (keV)	CED( $6^+$ ) (keV)	$\Delta E(8^+ \rightarrow 6^+)$ (keV)	CED( $8^+$ ) (keV)
$^{58}\text{Cu}$	1450	-4	1097	-12				
$^{58}\text{Ni}$	1454		1105					
$^{62}\text{Ga}$	1017	+63	1217	+48				
$^{62}\text{Zn}$	954		1232					
$^{66}\text{As}$	964	+7	1222	+12				
$^{66}\text{Ge}$	957		1217					
$^{70}\text{Br}^a$	933	-12	1069	-24	(963)	-35	(1025)	-26
$^{70}\text{Se}$	945		1093		964		1034	
$^{74}\text{Rb}$	478	+22	575	+39	783	+54	[976] <sup>b</sup>	+63
$^{74}\text{Kr}$	456		558		768		967	

<sup>a</sup>Higher analog states were reported by de Angelis *et al.* [22] but later refuted in an experiment by Jenkins *et al.* [6].

<sup>b</sup>Tentative.

depression of the  $T = 1$  states relative to the many new  $T = 0$  levels can be taken as clear evidence of  $T = 1$   $np$  pairing, as originally suggested by Rudolph *et al.* [14] and the apparent absence of any low-lying  $J^\pi = 1^+$  state an indication of the suppression of  $T = 0$  pairing at low spin [20].

Coulomb energy differences (CEDs) are defined as  $\Delta = E(J : T = 1, T_z = 0) - E(J : T = 1, T_z = -1)$ . All the states in  $^{74}\text{Rb}$  are higher in energy than their  $^{74}\text{Kr}$  counterparts, so the CEDs are all positive. In general, this shift is opposite what one would expect for Thomas-Ehrman- [1,2] type binding energy shifts; the  $T_z = 0$  nucleus lying closer to the proton dripline so having less binding energy and consequently having more extended proton wave functions and lower Coulomb energy. In the next lightest odd-odd  $N = Z$  nucleus, de Angelis *et al.* [22] found candidate states for the  $^{70}\text{Br}$  analogs of  $^{70}\text{Se}$  to spin  $J = 8$  that all fell below the  $^{70}\text{Se}$  levels. They suggested that for  $^{70}\text{Br}$  the negative CEDs could be attributed to such a Thomas-Ehrman effect. However, Jenkins *et al.* [6] questioned these assignments, as the states could not be observed in a similar, though higher statistics, data set. Table III shows the systematic trends in the  $fp$ g shell above  $^{56}\text{Ni}$ . Beyond  $A = 74$  no  $T = 1$  excited states are known in any odd-odd nuclei, although experiments on  $^{78}\text{Y}$ ,  $^{82}\text{Nb}$ , and  $^{86}\text{Tc}$  are currently in progress [39,40]. It is clear that there is no trend that simply follows binding energy. As far as testing wave functions for CVC  $\beta$ -decay physics the trends are reassuring in the sense that the shifts all appear modest and the Coulomb distortion small. However, it is an interesting open challenge to perform a shell-model calculation to try to reproduce the observed CEDs above  $^{56}\text{Ni}$  and understand their underlying cause.

### B. The new $T = 0$ states in $^{74}\text{Rb}$

The original yrast line of  $^{74}\text{Rb}$  proposed by Rudolph *et al.* [14] is irregular in its level spacing, and the poor population of nonyrast states makes it very difficult to isolate any bands and fathom their underlying structure. The new levels found in the present work go some way toward classifying the levels into

groups with distinctly different structure. The decay scheme in Fig. 1 emphasizes this grouping and highlights the fact that the irregular yrast line at low spin arises from several changes in structure.

### 1. The $K = 3$ Band

O’Leary *et al.* [15] pointed out that the sequence immediately above  $J = 3$  (structure 2 in Fig. 1) had the only  $\Delta J = 1$  decays seen in this nucleus, which they inferred to be pure  $M1$  decays, based on DCO ratio analysis. They attributed a distinct prolate Nilsson configuration,  $[312]_{\frac{3}{2}}$ , occupied by the unpaired proton and neutron. They supported this suggestion by a strong-coupling branching-ratio analysis that allowed them to deduce a magnetic moment for the band. They found it to be consistent with their suggested Nilsson assignment. Another separate analysis, using the two-quasiparticle rotor model [41], concluded that this band is much more complex, with contributing amplitudes from many Nilsson configurations.

We have extended the band, possibly to the  $J = 9$  member, so can further test the inferences of these models. Only the  $E2$  cascades could be followed, and no further  $\Delta J = 1$  decays were observed despite a careful search. We have calculated the branching ratios expected for this band assuming constant structure, that is, assuming the electromagnetic properties remain constant and using the experimentally observed  $\gamma$ -ray transition energies. For a band of fixed quadrupole moment, and zero magnetic moment, there will be  $\Delta J = 1$  and  $\Delta J = 2$   $E2$  matrix elements competing in a ratio reflecting phase-space and Clebsch-Gordan coefficients [42]. For the  $J = 5$  member where the experimental 482- to 264-keV branching ratio is  $\sim 20(5)\%$ , a pure  $E2$  ratio of  $\sim 28\%$  is predicted. This appears to leave no room for any  $M1$  contribution at all. We were able to measure the angular distribution of the 264-keV transition and found it to be neither pure dipole nor pure quadrupole but to have a multipole mixing ratio,  $\delta = 0.3(2)$ , suggesting considerable  $E2/M1$  mixing. This is clearly internally inconsistent, as in the strong coupling limit

this  $M1$  contribution would make the  $\Delta J = 1$  and  $\Delta J = 2$  branches almost equal in intensity, far from what is observed in any of our three data sets. This type of inconsistency appears to rule out any interpretation of these states as a simple strong-coupled Nilsson band. It does suggest that the band has a small magnetic moment, suppressing  $\Delta J = 1$  decays. The failure to observe higher lying  $\Delta J = 1$  branches is consistent with a small magnetic moment for the states, but mainly reflects the increased phase space for the  $E2$ ,  $\Delta J = 2$  crossover transitions. A small magnetic moment for a band can arise from significant proton and neutron occupancy of a “folded” configuration, like the  $[312]_{\frac{3}{2}}^3$  Nilsson state of spherical  $f_{\frac{7}{2}}$  parentage, but our observations suggest that the structure is changing on a state-by-state basis.

Another manifestation of structural evolution with spin lies in the moment of inertia of the band. The sequence of levels has a moment of inertia that rises with spin, a feature that is common in the  $A \sim 80$  region. However, the  $J = 7$  member of the band is displaced from its location based on any smooth increase of moment of inertia. It is depressed in energy by about 50 keV. One may speculate that this displacement comes from mixing with another, unobserved but expected,  $J^\pi = 7^+$  level, arising from  $g_{\frac{9}{2}}$  proton-neutron parentage. The depression of the  $J^\pi = 7^+$  member of the  $K = 3$  band would be matched by an elevation of the other state, to a location close to the  $J^\pi = 9^+$  level at 2309 keV, so its population would be small and detection very difficult. Apart from displacing the states, such mixing would introduce a significant  $g_{\frac{9}{2}}$  proton-neutron component into the 2007-keV state that would remove any significant  $K$  hindrance in the 303-keV decay between the 2309-keV,  $J^\pi = 9^+$  aligned band head and the 2007-keV,  $J^\pi = 7^+$  state. Isomeric  $J^\pi = 9^+$  states in  $^{66}\text{As}$  and  $^{70}\text{Br}$  were recently discussed by Hasegawa *et al.* [43]. Unlike the case in  $^{70}\text{Br}$  that has a  $J^\pi = 9^+$ , 2.19(9)-s isomer at 2293 keV [21,44] and that has no low multipole  $\gamma$ -decay path so  $\beta$  decays, or  $^{66}\text{As}$ , which has an 8.2(5)- $\mu\text{s}$  isomer [45],  $^{74}\text{Rb}$  has a favored path and a relatively uninhibited quadrupole decay.

## 2. The band based on $g_{9/2}$ occupancy

Above  $J^\pi = 9^+$  a long sequence of states (band 4 of Fig. 1) proceeds to high spin. The states do not form a very smooth sequence with near-constant moment of inertia, as one finds in the best nuclear rotors, which suggests the structure is continually evolving with spin. Such competition for dominance of the yrast line has been seen in neighboring even-even nuclei and may reflect the lack of a single energetically favored shape [46]. O’Leary *et al.* [15] found a candidate even-spin positive-parity sequence (band 3 in their work) that was suggested to be the rotationally aligned signature partner band. Our analysis shows the sequence contains a 730-keV transition as part of the main cascade, instead of being a sidebranch as they suggested. This observation considerably alters the moment of inertia, making a more regular match with the odd-spin sequence, with good interleaving of the high-spin level energies.

Unlike the  $K = 3$  band no intraband  $\Delta J = 1$  decays were observed at all between the high-spin sequences, despite a careful search. O’Leary *et al.* [15] suggested this arises for

several reasons. In a fully aligned  $\pi g_{\frac{9}{2}} \nu g_{\frac{9}{2}}$ ,  $J = 9$  configuration the proton and neutron magnetic vectors largely cancel, making the overall magnetic moment of the band relatively low and thus the  $M1$  in-band matrix elements small. The phase space for high-energy transitions favors the in-band  $E2$  decays. Finally, as this is an  $N = Z$  nucleus, and a  $T = 0$  band, all dipole transitions are suppressed [37,47], further reducing the  $E2$  vs.  $M1$  competition. In the future, it is important to obtain a larger data set and measure lifetimes to quantify these matrix elements and put the suppression on a quantitative footing.

## 3. The new band

A new band, band 5 in Fig. 1, was observed in this work. It decays only to the first excited state and so required good channel selection to confirm it is indeed a  $^{74}\text{Rb}$  cascade. The first two transitions are difficult to order, but whatever their sequence, this is the lowest-lying structure after the  $T = 1$  analog ground-state band. Initially, because of its low energy, we considered the possibility this could be an analog of the  $J = 0$  or  $J = 2$  band heads in  $^{74}\text{Kr}$  (see below), but there is no supporting evidence for such an assignment and the observed decay pattern is quite unlike these levels in  $^{74}\text{Kr}$ .

Two possible scenarios have been discussed. O’Leary *et al.* [15] suggested that if there were *two* low-lying positive-parity even-spin bands it would suggest the absence of a  $T = 1$  neutron-proton pair field. Thus, if this band has even spin and positive parity, it would be a candidate band that would undermine much of what we know about neutron-proton correlations in this region. However, the 248-keV angular distribution has a near-isotropic angular distribution, so our data slightly favor an odd-spin sequence. An alternative interpretation, also discussed by O’Leary *et al.* [15], is the possibility of a  $K = 1$  negative-parity band at relatively low excitation. Our new band has properties more in line with this hypothesis, though it is not clear why it lies so low in energy.

## C. Search for the $J = 0$ isomer in $^{74}\text{Rb}$

The location of the analog of the low-lying  $J^\pi = 0^+$  isomer that lies at 508 keV in  $^{74}\text{Kr}$  is important. We looked for delayed  $\gamma$  rays in  $^{74}\text{Rb}$  that might be expected from such an isomer, particularly a low-energy transition in coincidence with the 478-keV decay from the first excited state. There were no clear candidates in any of the data sets, though the experiment with the FMA had no Microball to attenuate low-energy transitions and was sensitive to low-energy (20- to 50-keV) decays from a 1- to 10-ns isomer. The Microball data sets were more restricted in sensitivity for low-energy  $\gamma$  rays, as has been discussed by Devlin *et al.* [48].

We considered that the 248-keV  $\gamma$  ray in the new band may come from a state directly above the 478-keV level and thus could be from a candidate  $J = 0$  level at 726 keV. If the  $J = 0$  shape-isomeric state really was so highly excited it would decay mainly to the  $J = 2$  level and have a lifetime on the  $\sim$  nanosecond level. However, several factors discourage this hypothesis. First, above this state lies a band of coincident  $\gamma$  rays that are well populated to high spin. This is completely unlike the situation in  $^{74}\text{Kr}$ , where it has been remarkably



difficult to populate any states feeding into that isomer [29]. If the band head has spin  $J = 0$  all the band members are very nonyrast and it is difficult to understand why they should be so well populated. Second, the 248- and 478-keV decay sequence would form a  $J = 0 \rightarrow 2 \rightarrow 0$  cascade. Such a spin combination has a unique and strongly peaked opening angle correlation, independent of alignment, as only the  $m = 0$  magnetic substate is involved. In our data the events seemed uniformly spread in opening angle, so, although the statistics were poor, the hypothesis seems unlikely. Finally, a 726-keV,  $J^\pi = 0^+$  state would suggest a Coulomb energy difference of 218 keV, which seems improbably large.

Our failure to identify  $\gamma$  rays from the  $J^\pi = 0^+$  isomer leads us to believe that its location is close to 500 keV and thus the  $\gamma$  branch to the  $J = 2$  state is suppressed to a point where the decay is all, or almost all, by internal conversion. In heavy-ion reactions, the  $^{74}\text{Kr}$  isomer is poorly fed by cascades from high spin, and it is likely the situation is similar or, even worse, in  $^{74}\text{Rb}$  as the extra  $T = 0$  states carry most of the  $\gamma$ -ray flux from high spin. Nonetheless, it would be very interesting to perform an experiment to search for delayed ( $\sim 30$  ns)  $E0$  conversion electrons from this state and find this important analog level.

#### IV. CONCLUSION

The spectrum of excited states in  $^{74}\text{Rb}$  has been extended using data from several Gammasphere experiments. Cold, near-barrier heavy-ion fusion reactions were important for finding nonyrast states. Most importantly, the ground-state  $T = 1$  rotational band has been extended to a candidate

$J = 8$  state. These levels are the analogs of the  $^{74}\text{Kr}$  ground-state sequence and demonstrate rather small Coulomb energy differences which have a trend opposite to Thomas-Ehrman shifts. The observation of new nonyrast states has allowed the very irregular  $T = 0$  deexcitation cascade from high spin originally found by Rudolph *et al.* [14] to be grouped into bands. These observations help clarify the location of excited configurations. A new band was observed. Together, these observations emphasize the unusual nature of odd-odd  $^{74}\text{Rb}$  as having a clear  $T = 1$  pairing “gap” between the ground-state and quasiparticle excitations, similar to the situation found in even-even nuclei. A careful search was made for a low-lying  $J^\pi = 0^+$  isomer, analogous to that known in  $^{74}\text{Kr}$ , but no candidate was identified. It may be that a new type of experiment, involving tagging on the ground-state decay with the recoil beta tagging (RBT) technique [49], could be very sensitive to selecting this and other low-lying states.

#### ACKNOWLEDGMENTS

This work involved several experiments over a period of years. More than three dozen scientists from the Gammasphere community were involved in some phase of data collection for this research and we thank them all. Analysis was facilitated by the strong Gammasphere infrastructure, which has remained stable over a decade, allowing easy comparison of data. This research was supported in part by the Department of Energy, Office of Nuclear Physics under contracts W-109-31-ENG38 (ANL) and DE-AC05-00OR22725 (ORNL), and grant DE-FG05-88ER40406 (Washington University), and by NSF research grants PHY95-14157 (Pennsylvania) and PHY-0244895 (DePaul).

- 
- [1] R. G. Thomas Phys. Rev. **81**, 148 (1951); **88**, 1109 (1952).
  - [2] J. B. Ehrman, Phys. Rev. **81**, 412 (1951).
  - [3] J. A. Nolen and J. P. Schiffer, Annu. Rev. Nucl. Sci. **19**, 471 (1969).
  - [4] S. M. Lenzi *et al.*, Phys. Rev. Lett. **87**, 122501 (2001).
  - [5] J. Ekman *et al.*, Phys. Rev. Lett. **92**, 132502 (2004).
  - [6] D. G. Jenkins *et al.*, Phys. Rev. C **72**, 031303(R) (2005).
  - [7] J. C. Hardy and I. S. Towner, Phys. Rev. Lett. **94**, 092502 (2005).
  - [8] D. H. Wilkinson, Nucl. Instrum. Methods A **543**, 497 (2005).
  - [9] C. Chandler *et al.*, Phys. Rev. C **56**, R2924 (1997); **61**, 044309 (2000).
  - [10] E. Bouchez *et al.*, Phys. Rev. Lett. **90**, 082502 (2003).
  - [11] J. M. D’Auria, L. C. Carraz, T. G. Hansen, B. Johnson, S. Mattsson, H. L. Ravn, M. Skarestad, L. Westgaard (ISOLDE Collaboration), Phys. Lett. **B66**, 233 (1977).
  - [12] P. H. Regan *et al.*, Acta Phys. Pol. B **28**, 431 (1997).
  - [13] M. Oinonen *et al.* Nucl. Phys. **A701**, 613c (2002).
  - [14] D. Rudolph *et al.*, Phys. Rev. Lett. **76**, 376 (1996).
  - [15] C. D. O’Leary *et al.*, Phys. Rev. C **67**, 021301(R) (2003).
  - [16] J. C. Hardy and I. S. Towner, Phys. Rev. Lett. **88**, 252501 (2002).
  - [17] A. V. Afanasjev and S. Frauendorf, Nucl. Phys. **A746**, 575c (2004).
  - [18] S. Glowacz, W. Satula, and R. A. Wyss, Eur. Phys. J. A **19**, 33 (2004).
  - [19] A. Petrovici, K. W. Schmid, and A. Faessler, Nucl. Phys. **A647**, 197 (1999).
  - [20] R. R. Chasman, Phys. Lett. **B577**, 47 (2003).
  - [21] D. G. Jenkins *et al.*, Phys. Rev. C **65**, 064307 (2002).
  - [22] G. de Angelis *et al.*, Eur. Phys. J. A **12**, 51 (2001).
  - [23] G. C. Ball *et al.*, Phys. Rev. Lett. **86**, 1454 (2001).
  - [24] A. Kellerbauer *et al.*, Phys. Rev. Lett. **93**, 072502 (2004).
  - [25] A. Piechaczek *et al.*, Phys. Rev. C **67**, 051305(R) (2003).
  - [26] M. Oinonen *et al.*, Phys. Lett. **B511**, 145 (2001).
  - [27] J. Heese, D. J. Blumenthal, A. A. Chishti, P. Chowdhury, B. Crowell, P. J. Ennis, C. J. Lister, and Ch. Winter, Phys. Rev. C **43**, R921 (1991).
  - [28] D. Rudolph *et al.*, Phys. Rev. C **56**, 98 (1997).
  - [29] F. Becker *et al.*, Eur. Phys. J. A **4**, 103 (1999).
  - [30] I. Y. Lee, Nucl. Phys. **A520**, 641c (1990).
  - [31] D. G. Sarantites, P.-F. Hua, M. Devlin, L. G. Sobotka, J. Elson, J. T. Hood, D. R. LaFosse, J. E. Sarantites, and M. R. Maier, Nucl. Instrum. Methods A **381**, 418 (1996).
  - [32] D. G. Sarantites *et al.*, Nucl. Instrum. Methods A **530**, 473 (2004).
  - [33] C. N. Davids *et al.*, Nucl. Instrum. Methods B **70**, 358 (1992).
  - [34] C. J. Gross *et al.*, Phys. Rev. C **56**, R591 (1997).
  - [35] R. Wadsworth *et al.* have analyzed a further data set on  $^{74}\text{Rb}$  that supports the original assignment of Ref. [15] (private communication).
  - [36] S. M. Fischer, T. Anderson, P. Kerns, G. Mesoloras, D. Svelnys, C. J. Lister, D. P. Balamuth, P. A. Hausladen, and D. G. Sarantites, Phys. Rev. C **72**, 024321 (2005).

- [37] A. Gelberg, A. F. Lisetskiy, R. V. Jolos, P. von Brentano, T. Otsuka, T. Sebe, and Y. Utsuno, *Prog. Theor. Phys. (Kyoto), Suppl.* **146**, 553 (2002).
- [38] A. F. Lisetskiy, A. Gelberg, R. V. Jolos, N. Pietralla, and P. von Brentano, *Phys. Lett.* **B512**, 290 (2001).
- [39] R. Wadsworth *et al.* at Jyvaskyla (private communication).
- [40] A. Garnsworthy *et al.* at GSI (private communication).
- [41] J. Uusitalo *et al.*, *Phys. Rev. C* **57**, 2259 (1998).
- [42] H. Morinaga and T. Yamazaki, *In Beam Gamma Spectroscopy* (North Holland, Amsterdam, 1976), p. 353.
- [43] M. Hasegawa, Y. Sun, K. Kaneko, and T. Mizusaki, *Phys. Lett.* **B617**, 150 (2005).
- [44] M. Karny, L. Batist, D. Jenkins, M. Kavatsyuk, O. Kavatsyuk, R. Kirchner, A. Korgul, E. Roeckl, and J. Zylicz, *Phys. Rev. C* **70**, 014310 (2004).
- [45] R. Grzywacz *et al.*, *Nucl. Phys.* **A682**, 41c (2001).
- [46] S. M. Fischer, C. J. Lister, and D. P. Balamuth, *Phys. Rev. C* **67**, 064318 (2003).
- [47] E. K. Warburton in *Isospin in Nuclear Physics*, edited by D. H. Wilkinson (North Holland, Amsterdam, 1970).
- [48] M. Devlin, L. G. Sobotka, D. G. Sarantites, and D. R. LaFosse, *Nucl. Instrum. Methods A* **383**, 506 (1996).
- [49] A. N. Steer *et al.*, *Nucl. Instrum. Methods A* **565**, 630 (2006).